

PAPER • OPEN ACCESS

## Four-point transient potential drop measurements on metal plates

To cite this article: Øyvind Persvik and Zhiliang Zhang 2020 *Meas. Sci. Technol.* **31** 024006

View the [article online](#) for updates and enhancements.

# Four-point transient potential drop measurements on metal plates

Øyvind Persvik<sup>1</sup>  and Zhiliang Zhang

Department of Structural Engineering, Norwegian University of Science and Technology (NTNU), 7491 Trondheim, Norway

E-mail: [oyvind.persvik@ntnu.no](mailto:oyvind.persvik@ntnu.no)

Received 19 August 2019, revised 29 September 2019

Accepted for publication 16 October 2019

Published 26 November 2019



## Abstract

The transient potential drop method is based on measurement of the transient voltage on the surface of a conductor due to the injection of a pulsed current. In this paper, we consider an approximate analytical model for four-point transient potential drop measurements on plates that are thin compared to the probe separation. Experimental results show good agreement with the theory for measurements made on non-magnetic and ferromagnetic plates when an exponentially rising pulsed current is used as a source. To demonstrate possible applications of the theory we consider measurement of the conductivity and relative permeability of the materials as well as plate thickness.

Keywords: transient potential drop, materials characterization, electromagnetic non-destructive evaluation, four-point probe

(Some figures may appear in colour only in the online journal)

## 1. Introduction

The four-point potential drop (PD) technique has been in use for more than a century in various fields, notably in geophysical and materials sciences [1] where it is a standard approach for measurement of the electrical resistivity of soil and semi-conductors. The technique is also used for the characterization of metals [2] and modern applications include the probing of micro-scale particles [3]. In four-point measurements, a current is injected into the material via electrical contacts and the voltage response is measured across one or more separate pairs of contacts. This arrangement achieves high sensitivity to the properties of the probed sample since the contact resistance between the sample and the current-carrying wires can be neglected. Figure 1 illustrates a four-point probe consisting of spring-loaded pins where the drive current is delivered via the two outer contacts and the inner pair of pins serves as the voltage probe.



Original content from this work may be used under the terms of the [Creative Commons Attribution 3.0 licence](https://creativecommons.org/licenses/by/3.0/). Any further distribution of this work must maintain attribution to the author(s) and the title of the work, journal citation and DOI.

<sup>1</sup> Author to whom any correspondence should be addressed.

In traditional applications, such as resistivity and crack measurement, the direct current potential drop (DCPD) method has been widely adopted and requires only a direct current source and the measurement of a steady voltage [1, 4]. Alternating current potential drop (ACPD) has been used for materials characterization [2] and crack measurement [5, 6] by exploiting the frequency-dependent skin depth of a time-harmonic injected current [4]. In contrast, the transient potential drop method relies on recording the transient response to a pulsed current. Physically, the resulting time-dependent skin effect voltage is due to the diffusion of quasi-static electromagnetic fields in the material excited by the pulsed drive current. The method has applications in non-destructive evaluation (NDE) of conducting materials, in particular for observing the variation of material properties or geometrical features with depth on the basis of the temporal evolution of the signals. In the analysis of such signals, where the goal is to deduce unknown properties of the material from the measurements, a general approach is the inversion of measurement data, a procedure that requires modeling of the sensor response by either analytical or numerical methods, or a combination these, and an important step in this development is the experimental validation of such models. With this in mind, we consider here the experimental validation of four-point

transient PD formulas for the fundamental case of measurements made on homogeneous plates.

In previous related work on four-point measurements, Bowler and Huang [7] used multi-frequency ACPD to measure the conductivity and magnetic permeability of homogeneous metal plates. As a model for variation of material properties with depth the theory of four-point ACPD on a layered half-space [8] has also been given. In other applications to NDE, Sposito *et al* used ACPD for measurement of material loss [9] and recently the application to stress monitoring by means of directional four-point probes was studied by Corcoran and Nagy [10].

Early work on transient PD was made by Hognestad and Honne [11] for measurement of tensile and compressive stresses in steel rods. More recently, theoretical evaluations were given for four-point transient PD measurements on planar half-space conductors [12] and plates [13] based on inverting the corresponding frequency-domain (ACPD) results [2]. However, these predictions have so far not been compared with experimental measurements to validate the theory and demonstrate its practical use. Although the existing literature on ACPD theory and experiment lends confidence to the validity of transient measurements, the latter requires in general that the time-dependence of the drive current is taken into account whereas in ACPD a simplification is made where the current is assumed to be sinusoidal with a given frequency. An analysis assuming a finite rise time of the drive current was given in [12] for transient four-point measurements on a half-space, but the analysis for plates in [13] was limited to the simplest case of an ideal step current.

In the present work we consider the experimental validation of four-point transient potential drop theory for measurements on plates that are thin compared to the probe spacing. In this context, a plate is considered thin when the plate thickness is less than one half of the probe separation, assuming equal separation between the probes [14]. With this restriction, the task of deriving the transient response is reduced to the analysis of a one-dimensional diffusion problem on the basis of time-domain equations. An advantage of this thin-plate approximation is that the results are expressed conveniently in terms of simple formulas which facilitate the interpretation of experimental data. Although the approximation for the transient step response on thin plates is also discussed in [13], where a (short-time) series solution is given, we consider here a solution to the diffusion equation on the form of an eigenfunction expansion to obtain an alternative formulation expressed as a steady state (DC) part and a summation term describing the transient response; in contrast, the short-time solution given in [13] is expressed as a half-space term, accurate at short time scales, together with image summations that correct for the finite thickness of the plate. Furthermore, we consider the response to an exponentially rising current pulse as a simple model for a drive current having a finite rise time. Finally, together with the experimental validation of these results, we discuss the use of the theory for measurement of conductivity, relative permeability and plate thickness.

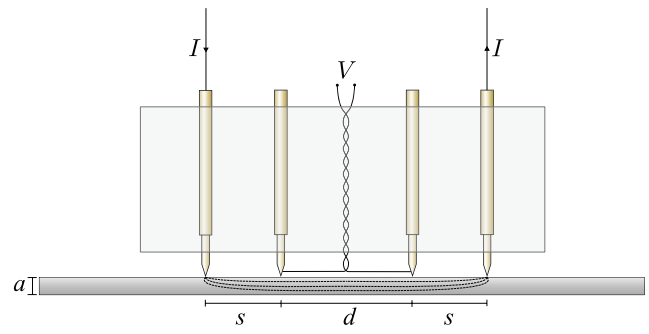


**Figure 1.** A four-point probe in contact with a metal plate of thickness  $a$ . The probes are co-linear and placed symmetrically about the mid-point of the probe. The spacing between each current injection pin and the nearest voltage probe is denoted by  $s$  and  $d$  is the separation between the voltage probes.

## 2. Theory of transient potential drop measurements

In potential drop methods a voltage difference  $V$ , measured between two points on the surface of a conducting material, is defined by the path integral

$$V = - \int_a^b \mathbf{E} \cdot d\mathbf{l} \quad (1)$$

where  $\mathbf{E}$  denotes the surface electric field vector due to a current flowing in the material. The potential is measured between two points  $a$  and  $b$  on the surface and  $d\mathbf{l}$  is an infinitesimal vector pointing along the integration path.

In general, the potential drop is a time-dependent voltage  $V(t)$  arising in response to a current  $I(t)$  which is assumed to be known. The DCPD and ACPD methods represent special cases where the applied current is either constant (DC) or alternating (AC) with a given frequency. In the former case a steady state voltage is measured while in the ACPD method a frequency-dependent voltage arises whose amplitude and phase are recovered by frequency-domain techniques such as lock-in amplification. In transient potential drop measurements the voltage due to a time-varying current is recorded and analyzed in the time domain. Typically, the current is a pulse which is initially zero and rises to a steady value, the simplest example of which is an ideal step current.

In the analysis of four-point measurements, it is customary to assume that the current is delivered via point contacts. Furthermore, given a time-varying source, we assume that the current is delivered by straight wires oriented perpendicular to the surface, ensuring that there is no inductive coupling between the current-carrying wires and the conducting material. The theoretical analysis involves first solving for the electromagnetic fields in the material due to a given current  $I(t)$ , and then calculating the potential from (1). Assuming that the fields are changing at slow rates, displacement currents can be ignored and Maxwell's equations reduce to diffusion equations for the quasi-static fields.

In the following we outline an approximate theory of four-point transient potential drop measurements on plates that are thin compared to the probe spacing. For completeness,

considering the limited literature on the transient PD method, we introduce the analysis in terms of one-dimensional magnetic field diffusion problems. Solutions to these problems are then used to express the transient voltage of a four-point probe.

### 2.1. Four-point potential drop due to steady current

Consider first the elementary case where a steady current is injected into a plate of thickness  $a$  and conductivity  $\sigma$ . Treating a single current source point in isolation, the fields are axially symmetric and the potential depends only on the radial distance from the source. The four-point potential drop can then be written as a superposition

$$V = V_+ + V_- \quad (2)$$

where  $V_+$  and  $V_-$  are the potential drops due to the positive and negative source points.

The analysis for thin plates or sheet material is simplified by considering only points sufficiently far away from the source points so that the current density is approximately uniform throughout the thickness of the plate. Conservation of the total current  $I$  over a cylindrical surface of radius  $r$  centered on the source gives the electric field  $E(r) = I/2\pi\sigma ra$  which may be integrated between two points  $r_1$  and  $r_2$  to get  $V = I \ln(r_2/r_1)/2\pi\sigma a$ . Adding the contribution from the negative source (or sink), the four-point probe voltage, according to (2), can be written as

$$V = \frac{I}{2\pi\sigma a} G \quad (3)$$

where  $G$  is a geometric probe factor. For arbitrary arrangement of the probes,  $G = \ln(r_2^+ r_1^- / r_1^+ r_2^-)$  with  $r_j^\pm$  denoting the distance from the positive (+) and negative (-) source to voltage probe  $j$ . For a co-linear probe, as in figure 1, with voltage probes separated by a distance  $d$  and letting  $s_1$  and  $s_2$  denote the separation of the source points and the voltage probes, the probe factor becomes

$$G = \ln \left[ \left( 1 + \frac{d}{s_1} \right) \left( 1 + \frac{d}{s_2} \right) \right]. \quad (4)$$

In the special case of a symmetric probe with  $s_1 = s_2 = s$ ,  $G = 2 \ln(1 + d/s)$  and for an equi-spaced probe,  $s = d$  and  $G = 2 \ln 2 \approx 1.4$ . Intuitively, the validity of the thin-plate approximation depends on the value of  $s$  since by making  $s$  small the voltage probe is moved closer to the source points where the assumption of uniform current does not hold [14]. The validity is examined in more detail later in relation to the transient potential drop.

### 2.2. Magnetic field diffusion in planar conductors

As a prototypical example of the transient potential drop method, consider the diffusion of a transient electromagnetic field into a homogeneous planar conductor [15] with linear conductivity  $\sigma$  and permeability  $\mu = \mu_0\mu_r$  where  $\mu_0$  is the free space permeability and  $\mu_r$  is the relative permeability of the material. The surface of the conductor is at  $z = 0$ , extends

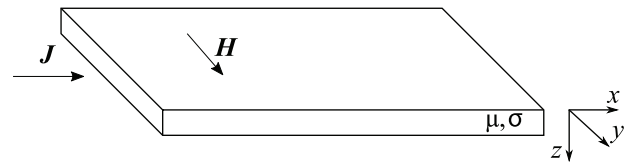


**Figure 2.** Orientation of the current density and magnetic field for the simple case of a current being injected into a planar conductor of finite thickness.

into the positive  $z$ -direction and is infinite in the lateral directions. A time-dependent current  $I(t)$ , flowing in the positive  $x$ -direction, gives rise to a current density  $\mathbf{J} = J(z, t)\hat{\mathbf{x}}$ , which is assumed to be uniform in the  $x$ - and  $y$ -directions.

This situation can be formulated as a one-dimensional magnetic field diffusion problem by considering the magnetic field  $\mathbf{H} = H(z, t)\hat{\mathbf{y}}$ , oriented perpendicular to the current density (figure 2), and whose magnitude at the surface,  $H_0$ , is related to the total current through Ampere's law,  $H_0 = I/w$  where  $w$  is the width of a square Amperian loop enclosing the current. In other words the surface magnetic field is in this case controlled by the total current per unit width. The current density  $J(z, t) = -\partial H/\partial z$  gives rise to a surface voltage per length  $l$  given by

$$\frac{V}{l} = -\frac{1}{\sigma} \frac{\partial H}{\partial z} \Big|_{z=0}. \quad (5)$$

The above relations between the the current density and the magnetic field are due to the differential form of Ampere's law,  $\nabla \times \mathbf{H} = \mathbf{J}$ .

To model transient fields, consider an initial-boundary value problem in terms of the magnetic field governed by the diffusion equation

$$\frac{\partial^2 H}{\partial z^2} = \mu\sigma \frac{\partial H}{\partial t} \quad (6)$$

with the initial condition  $H(z, 0) = 0$ , corresponding to zero current for  $t \leq 0$ , and the boundary condition  $H(0, t) = H_0(t)$  effectively taking into account the time-dependence of the current for  $t > 0$ . Assuming initially a half-space conductor we require also that  $H(z, t) \rightarrow 0$  for  $z \rightarrow \infty$ , reflecting the non-radiative nature of quasi-static fields.

A common solution method is to apply the Laplace transform defined by  $h(z, p) = \int_0^\infty H(z, t)e^{-pt} dt$  for the complex transform variable  $p$  [16]. Take the Laplace transform of (6) to obtain the ordinary differential equation

$$\frac{d^2 h}{dz^2} = \mu\sigma p h \quad (7)$$

with a solution that goes to zero as  $z \rightarrow \infty$  given by

$$h(z, p) = h_0(p)e^{-\sqrt{\mu\sigma p}z}. \quad (8)$$

Here,  $h_0(p)$  is the Laplace transform of the boundary condition. To find the response to an ideal step, write the boundary field as  $H_0(t) = H_0 u(t)$ , where  $u(t)$  is the Heaviside step function with Laplace transform  $1/p$ . Insert for  $h_0(p) = H_0/p$  into

(8) and take the inverse Laplace transform [17] to obtain the time-dependent field for  $t > 0$ ,

$$H(z, t) = H_0 \operatorname{erfc} \left( \sqrt{\frac{\mu\sigma}{4t}} z \right). \quad (9)$$

The resulting surface voltage is

$$V(t) = \frac{H_0}{\sigma} \sqrt{\mu\sigma/\pi t} \quad (10)$$

which decays to zero for  $t \rightarrow \infty$  reflecting the fact that the current density tends to zero as the total current is distributed throughout the half-space. Note that we implicitly assume zero fields for  $t \leq 0$  and therefore omit the unit step function  $u(t)$  in the expressions for  $H$  and  $V$ .

The magnetic field in (9) can be written in terms of a characteristic length scale  $\delta(t) = \sqrt{4t/\mu\sigma}$  representing a time-dependent diffusion depth analogous to the frequency-dependent skin depth in ACPD.

Next, assume that the material is bounded by an additional surface at  $z = a$ , corresponding to the bottom surface of a plate with thickness  $a$ . Initial and boundary conditions are as before except that now  $H(a, t) = 0$  meaning that the external source of the field is confined to the top surface as is typically the case in four-point potential drop measurements. We seek a solution for the transient potential on a form that decays to a steady state, which is appropriate for step-like drive currents that rise to a constant value. In other words, the solution should include a transient part that decays to zero for large values of  $t$ . A steady state solution of (6) that is zero at  $z = a$  takes the form  $1 - z/a$  with the omission of an integration constant. Assuming that  $h(z, p)$  is a solution to (7) with  $h(0, p) = h_0(p)$ , the transient field  $\bar{h}(z, p) = h(z, p) - h_0(p)(1 - z/a)$  fulfils the homogeneous boundary conditions  $\bar{h}(0, t) = \bar{h}(a, t) = 0$  and is a solution to the non-homogeneous equation

$$\frac{d^2 \bar{h}}{dz^2} - \kappa p \bar{h} = \kappa h_0(p) p (1 - z/a).$$

This permits a solution on the form of an eigenfunction expansion,

$$\bar{h}(p, z) = \sum_{n=1}^{\infty} A_n \sin(n\pi z/a). \quad (11)$$

The coefficients are determined by inserting for  $\bar{h}(p, z)$  into the differential equation and solving for  $A_n$ , which gives

$$A_n = -\frac{2h_0(p)p/k_n a}{k_n^2 + \mu\sigma p}$$

where  $k_n = n\pi/a$ . The full solution including the steady state part may then be written as

$$h(p, z) = h_0(p) \left( 1 - \frac{z}{a} - 2 \sum_{n=1}^{\infty} \frac{p \sin(k_n z)/k_n a}{k_n^2 + \mu\sigma p} \right). \quad (12)$$

Assuming a step change,  $h_0(p) = H_0/p$ , the magnetic field in the plate can be evaluated using elementary inverse Laplace transforms [17] with the result

$$H(z, t) = H_0 \left( 1 - \frac{z}{a} - 2 \sum_{n=1}^{\infty} \frac{\sin(k_n z)}{k_n a} e^{-k_n^2 t/\mu\sigma} \right). \quad (13)$$

Finally, taking the derivative with respect to  $z$  and evaluating the result at  $z = 0$  gives the surface potential,

$$\frac{V(t)}{l} = \frac{H_0}{\sigma a} \left( 1 + 2 \sum_{n=1}^{\infty} e^{-k_n^2 t/\mu\sigma} \right).$$

### 2.3. Four-point transient potential drop on thin plates

Consider now that a current  $I(t)$  is delivered to the plate via a single wire, resulting in an axially symmetric magnetic field that depends on the radial distance  $r$  from the wire in addition to  $z$  and  $t$ . Write the magnetic field as  $\mathbf{H} = H(r, z, t) \hat{\phi}$  where  $\hat{\phi}$  is a unit vector in the azimuthal direction in a cylindrical coordinate system centered on the current wire. Let  $H_0(t)$  denote the field in air surrounding the wire which is also the field at the plate surface and given by

$$H_0(t) = I(t)/2\pi r. \quad (14)$$

A simplified analysis of the fields inside the conductor can be made by making the assumption  $J_z = 0$ , i.e. the current density has only a radial component,  $\mathbf{J} = J(r, z, t) \hat{r}$ . Ampere's law,

$$\mathbf{J} = \frac{1}{r} \frac{\partial(rH)}{\partial r} \hat{z} - \frac{\partial H}{\partial z} \hat{r},$$

implies  $J = -\partial H/\partial t$  and that  $H \sim 1/r$ . A one-dimensional diffusion equation for  $H$  is then obtained by taking the partial derivative of  $J$  with respect to  $z$  and inserting into Faraday's law which may now be written as  $\partial J/\partial z = -\mu\sigma \partial H/\partial t$ . The resulting diffusion equation for  $H$ , given by (6), has the solution (13) except with  $H_0$  as in (14) which now ensures the required continuity of the tangential component of the magnetic field across the top plate surface.

The fact that the spatial and temporal dependence are separated means that we may simply write down the four-point transient step response as

$$V(t) = V_0 \left( 1 + 2 \sum_{n=1}^{\infty} e^{-\pi^2 t/\kappa_n} \right) \quad (15)$$

with  $V_0$  given by (3) and where we have defined  $\kappa_n = \mu\sigma a^2/n^2$ . In obtaining (15), only the  $1/r$ -dependence in (14) is integrated and the result summed to give  $V_0$ , as in section 2.1, with the other factors treated as being constant, including the time-dependent part. The first term in the series is the DC potential drop due to a steady current  $I_0$  and the exponential terms in the summation represent a transient skin effect voltage. Each additional term included in this series improves the accuracy at progressively shorter timescales.

### 2.4. Thin-skin approximation

The thin-plate approximation (15) can be applied to conductors of arbitrary thickness in the so-called thin-skin regime

where the diffusion depth of the current, rather than the plate thickness, is somewhat less than the probe spacing. The choice of  $a$  must be made to ensure that  $\delta(t) \ll a$  for this approximation to be valid. Here,  $a$  does not necessarily represent a physical boundary, but instead the assumption that  $H \approx 0$  at  $z = a$  artificially truncates the conducting region and enables the eigenfunction expansion in (11) [18].

Although (15) can be made accurate at short times by including enough summation terms, an exact expression for the thin-skin approximation is found by noting that the half-space result in (10), with similar reasoning as in the previous section, can be used to write the four-point potential drop as

$$V_{\text{ts}}(t) = \frac{I_0 G}{2\pi\sigma} \sqrt{\frac{\mu\sigma}{\pi t}}. \quad (16)$$

### 2.5. Finite rise time

The idealized step response diverges for  $t \rightarrow 0$ , which is immediately clear from (16), but in practice the response is limited due to the finite rise time of the drive current. Experimentally, the rise time may be controlled deliberately or limited by the finite bandwidth of the current drive circuitry. As a simple model of a step-like drive current of finite rise time, we consider the case of an exponentially rising current,

$$I(t) = I_0 \left(1 - e^{-t/\tau}\right), \quad (17)$$

which has the Laplace transform

$$\tilde{I}(p) = I_0 \left(\frac{1}{p} - \frac{1}{p + 1/\tau}\right).$$

To find the potential drop, use (12) and (5) to write the transform of the voltage as

$$v(p) = \frac{\tilde{I}(p)}{2\pi\sigma a} \left(1 + 2 \sum_{n=1}^{\infty} \frac{p}{k_n^2 + \mu\sigma p}\right).$$

After inserting for  $\tilde{I}(p)$  and expanding the terms inside the summation into partial fractions, inversion to the time domain gives

$$V_{\text{exp}}(t) = V_0 \left(1 - e^{-t/\tau} + 2 \sum_{n=1}^{\infty} \frac{e^{-t/\kappa_n} - e^{-t/\tau}}{1 - \tau/\kappa_n}\right). \quad (18)$$

Figure 3 shows this expression compared with the step response (15) and illustrates how controlling the rise time of the drive current limits the peak height of the transient.

The terms outside the summation in (18) are proportional to the drive current and may be considered a resistive contribution to the potential drop as it is present in the absence of any skin effect. In figure 4 this contribution is compared with the skin effect voltage.

The validity of the thin-plate approximation is indicated in figure 5 where it is shown that the error in the approximation can be made negligible (less than 0.2%) by measuring the potential at a distance  $s$  from the source points greater than approximately 2 times the plate thickness. In all cases the error

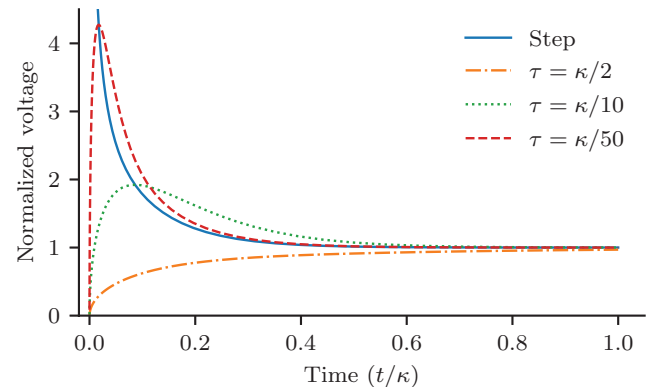


**Figure 3.** Transient potential drop due to an exponentially rising drive current for different values of the rise time  $\tau$  relative to the decay time constant  $\kappa = \mu\sigma a^2$ . The solid line shows the step response (15) corresponding to an ideal step change of the drive current and representing the limit  $\tau \rightarrow 0$ .

is zero at  $t = 0$  and remains negligible throughout the time range where the thin-skin approximation holds. Physically, the departure from the thin-skin regime reflects the influence of the probe distance  $s$  on the decay of the transient [13].

It is useful to also evaluate the response to a drive current having a finite rise time for the thin-skin approximation (16). In this case an exponential current pulse leads to transforms that are more complicated, but the result can be written compactly as

$$V_{\text{ts,exp}}(t) = \frac{I_0 G}{2\pi\sigma} \sqrt{\frac{\mu\sigma}{\tau}} D\left(\sqrt{t/\tau}\right). \quad (19)$$

Here,  $D(x)$  is the Dawson function [17] which is related to the error function by  $D(x) = (\sqrt{\pi}/2)e^{-x^2} \text{erfi}(x)$  where  $\text{erfi}$  is the imaginary error function defined by  $\text{erfi}(x) = -\text{ierf}(ix)$  which is a real function for real argument  $x$  despite the appearance of the imaginary unit. The actual Laplace inversion is carried out in the appendix.

### 3. Experiment

Transient potential drop measurements were made using a co-linear probe consisting of four spring-loaded pins held in place by plastic supports. The probe dimensions are given by  $s_1 = 7.5$  mm,  $s_2 = 10.5$  mm and  $d = 16.5$  mm, corresponding to a probe factor  $G \approx 2.1$  and an overall probe length of 34.5 mm. The separations between the probes were measured to within  $\pm 0.2$  mm using a mechanical ruler with .5 mm divisions. The drive current was generated by programming an arbitrary waveform generator (AWG) to produce a pulse train with exponentially rising and falling edges. By recording the response to several consecutive pulses, the resulting repetitive signal can be averaged to reduce random noise when appropriate.

A multi-channel PC oscilloscope was used to record both the drive current and the transient potential drop. The former was obtained by measuring the voltage over a precision resistor in series with the drive circuit; the transient potential drop on the plate was measured as the differential voltage

**Table 1.** Dimensions of the samples used in the experimental measurements. The accuracy of the thickness measurement is  $\pm 0.01$  mm.

Sample	Thickness	Width (mm)	Length
Aluminium	3.02	400	400
Steel (S235)	2.96	350	350
Steel sheet	1.21	400	500

between pick-up wires that were soldered close to the tips of the voltage probes and kept close to the plate surface to minimize the induced voltage in the loop formed by the wires and the conducting path between the probes. See also figure 6 for a schematic diagram of the experimental setup.

In the theory it is assumed that the current wires are infinitely long, although in practice the wires must form a closed loop and were extended for approximately 30 cm above the plate to minimize the influence of the inductive coupling between the plate and the sections of wire running parallel to the plate surface.

In addition to the potential drop due to the current in the plate there is another contribution to the measured voltage which is due to the mutual inductance between the vertical current wires and the pick-up probes. This voltage can be written as  $V_L = L di/dt$  where the inductance  $L$  is a geometrical parameter characteristic of the probe. For an exponentially rising current the induced voltage appears as an additive term on the form

$$V_L(t) = \frac{LI_0}{\tau} e^{-t/\tau}. \quad (20)$$

### 3.1. Materials

Three different samples were used in the experimental measurements: two plates, made of aluminium and carbon steel (grade S235), both having a nominal thickness of 3 mm, and a somewhat thinner sample of DC01 cold-rolled steel sheet with a nominal thickness of 1.2 mm. The thickness of each sample was measured more accurately using a micrometer and taking the average of readings at several points along the plate edges. The dimensions of the samples are summarized in table 1.

The samples are wide compared to the probe length to minimize edge effects: all samples have lateral dimensions greater than ten times the probe length which reduces the expected DC error due to edge effects to less than 1% [19].

### 3.2. Permeability and thickness measurement

In section 2.5 it is shown that the transient potential drop, (18), can be expressed in terms of the constant DC voltage  $V_0$  and a transient part characterized by the decay time-constant  $\kappa = \mu\sigma a^2$  and the rise time  $\tau$  of the drive current. In the following we use the probe resistance defined by  $R = V_0/I_0$ , which may be written in terms of the probe and plate parameters as  $R = G/2\pi\sigma a$ . Experimentally, the probe resistance is determined from the DC voltage  $V_0$  which is extracted from the measured voltage pulse after it reaches a steady state. The transient decay time is then determined in a fitting procedure

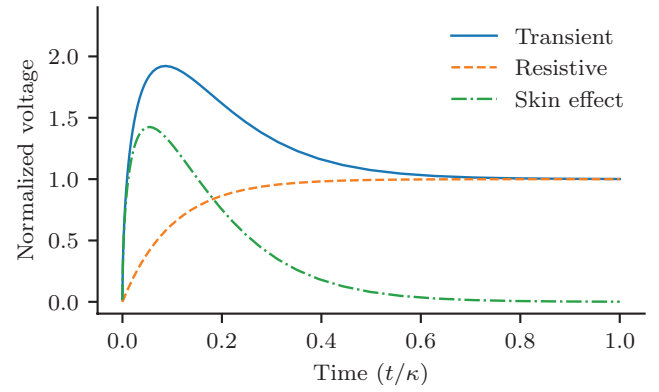


**Figure 4.** A transient voltage decomposed into resistive and skin effect contributions for a rise time  $\tau = \kappa/10$ . The resistive part is proportional to the exponential drive current. The skin effect contribution is due to the magnetic excitation of the material and its peak height determined by the rise time.

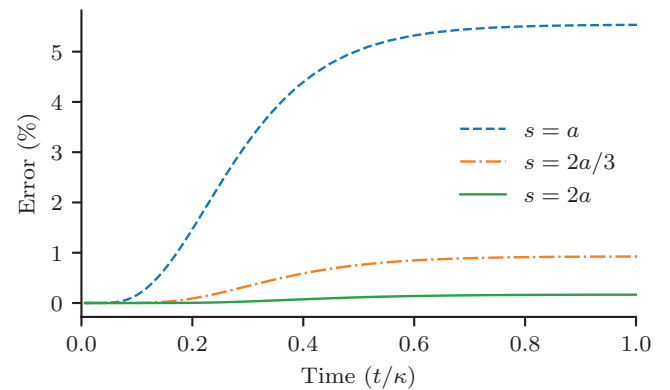


**Figure 5.** Validity of the thin-plate formula indicated by the percentage difference between the transient step response calculated using the thin-plate approximation and the formula for plates of arbitrary thickness given in [13]. A symmetric probe with  $d = 2s$  was assumed in the calculations.

where a value of  $\kappa$  in (18) is found that minimizes the residual sum of squares between the measured potential drop and the theoretical prediction.

From the experimental values of  $R$  and  $\kappa$ , the model parameters  $\mu$ ,  $\sigma$  and  $a$  can be determined. Assuming first that the thickness is known, the conductivity is given by

$$\sigma = G/2\pi Ra \quad (21)$$

and the relative permeability can be found either from  $\mu_r = \kappa/\mu_0\sigma a^2$  using the estimate of  $\sigma$  or directly in terms of the measured parameters according to

$$\mu_r = 2\pi\kappa R/\mu_0 a G. \quad (22)$$

Alternatively, both the conductivity and the thickness can be determined simultaneously assuming that the permeability is known, for example in measurements made on non-magnetic materials with  $\mu_r = 1.0$ . Taking the product  $\kappa R^2$  to first eliminate  $a$  gives the conductivity,

$$\sigma = G^2\mu/4\pi^2 R. \quad (23)$$

Similarly,  $\sigma$  is eliminated by taking the product  $\kappa R$  to get the thickness,

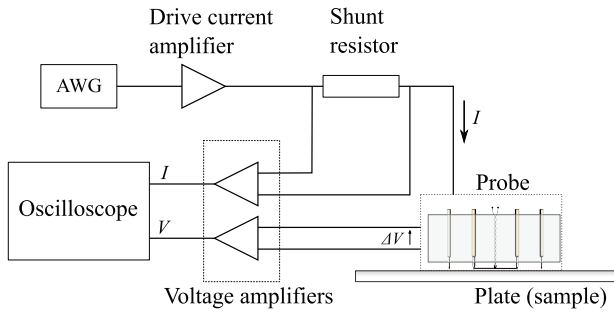


**Figure 6.** Simplified schematic diagram of the measurement setup. The drive current waveform generation and the oscilloscope recordings are controlled from a PC.

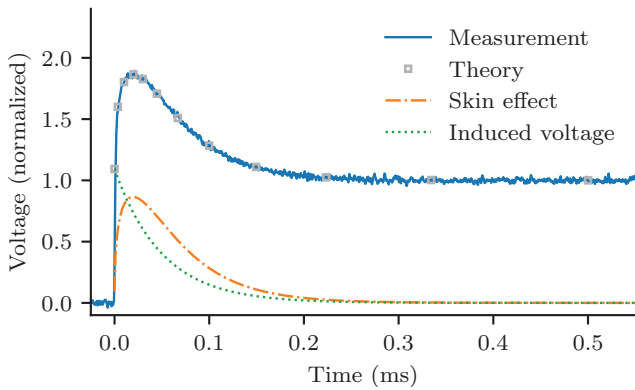


**Figure 7.** Transient potential drop measurement on the aluminium plate. The experimental measurement is given by the solid line and the grey squares represent the theoretical calculation. The estimated contributions from the skin effect voltage and the induced voltage are also shown to indicate the relative magnitude of these effects.

$$a = 2\pi\kappa R/G\mu. \quad (24)$$

These formulas are applied in the following sections for the interpretation of the experimental measurements.

The principle of conductivity and permeability measurement outlined above is similar to the procedure by Bowler and Huang [7] using multi-frequency ACPD. However, although application of the theory to thickness measurement was also considered in their work, an independent measurement of the conductivity was used instead of determining both parameters from the potential drop data.

Note that the most direct approach to the analysis presented above is to include a sufficient number of summation terms in the calculations of (18) to accurately describe the entire measured transient. However, a practical simplification is to include only a few terms in the calculations and restrict the analysis to the late part of the decay where the resulting approximation is valid. For example, in the simplest case, the transient voltage is described by a single exponential according to (15) provided that the rise time of the current is short relative to the transient decay time (figure 3). Moreover, in this limit where the transient response approaches the step response the measurement is made independent of the exact form of the drive current.

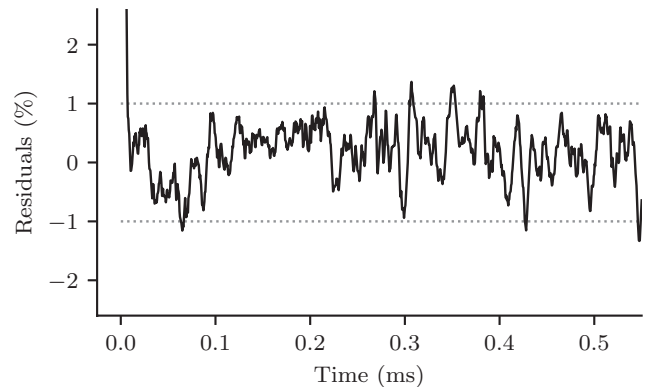


**Figure 8.** Residuals in the fit for the aluminium plate in figure 8 plotted as the percentage error relative to the DC value of the measured potential drop.

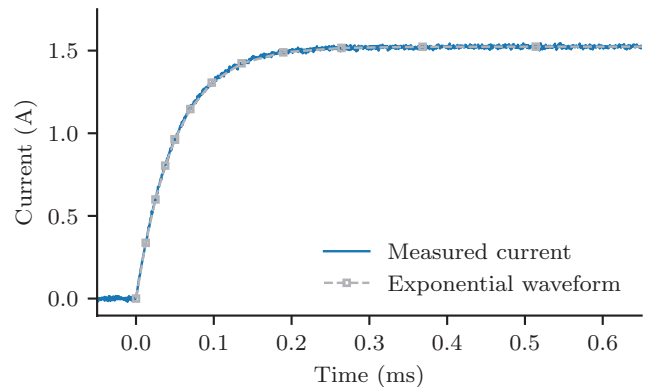


**Figure 9.** Measured current in the aluminium plate compared with the prescribed exponential waveform having a rise time of 50  $\mu\text{s}$ .

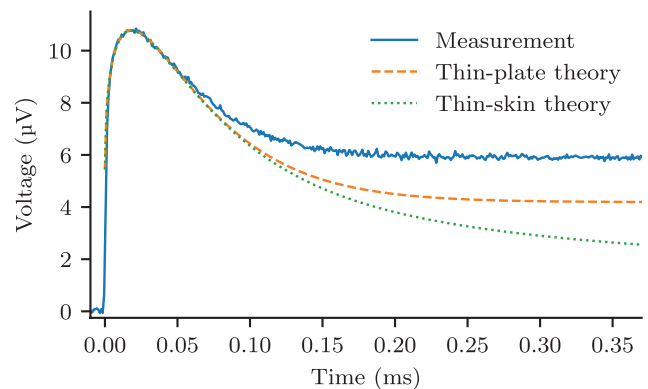


**Figure 10.** Measurement on the aluminium plate when the probe separation is less than the plate thickness and the thin-plate approximation does not hold. The thin-plate theory (18) and thin-skin theory (19) are plotted using a conductivity of 19.0  $\text{MS m}^{-1}$ .

### 3.3. Aluminium plate measurements

Figure 7 shows experimental data from a transient potential drop measurement on the aluminium plate, together with the theoretical prediction calculated from (18) using parameters obtained in the fit procedure. Also shown is the contribution from the induced voltage ( $L = 0.32 \text{ nH}$ ) along with the skin effect voltage which illustrates that the induced voltage

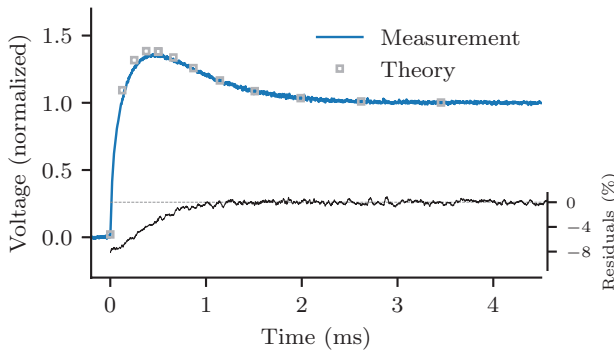


**Figure 11.** Transient potential drop measurements on the 3 mm thick steel plate. A drive current with amplitude 500 mA and a rise time of 0.5 ms was used. The inset shows the normalized residuals between the measured transient and the theoretical calculation.

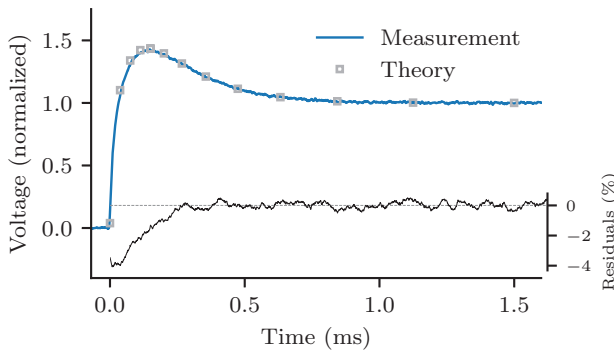


**Figure 12.** Transient potential drop measurement on the steel sheet with thickness 1.2 mm. The drive current has a magnitude of approximately 200 mA and a rise time of 165  $\mu$ s.

contributes a significant fraction of the overall transient voltage.

An average of 64 pulses was used to obtain residuals (figure 8) within about  $\pm 1\%$  for the duration of the transient. The residuals are given as the difference between the theoretical and measured normalized voltages. As such, they represent the percentage difference relative to the DC potential drop. The drive current, with magnitude 1.5 A and rise time 40  $\mu$ s, is shown in figure 9 and compared with the prescribed exponential waveform.

The measurement corresponds to a conductivity of  $19.0 \pm 0.5 \text{ MS m}^{-1}$  and a relative permeability of  $0.98 \pm 0.03$ , calculated from (21) and (22) using the known thickness of the plate together with the measured probe resistance of  $5.95 \mu\Omega$  and a decay time constant of 214  $\mu$ s obtained in the fit. The accuracy of approximately 3% in the parameter estimates are evaluated by propagation of error in the respective formulas where the main contributions are due to uncertainties in the resistance measurement and the probe factor.

Following the discussion in the previous section, the thickness and the conductivity can be estimated from the measurement data by setting  $\mu_r = 1.0$ , which gives  $\sigma = 19.3 \pm 0.7 \text{ MS m}^{-1}$  and  $a = 2.97 \pm 0.09 \text{ mm}$  calculated from (23) and (24). The higher uncertainty in this conductivity estimate compared to that above is due to the probe factor appearing in the second power in the corresponding expression for  $\sigma$ .

In the present context, estimates of the relative permeability and plate thickness serve as useful checks on the validity

of the theory since both parameters are known. However, the approach also allows for simple measurement of the thickness of planar conductors without the need for an independent conductivity measurement.

#### 3.4. Thin-skin measurement

Figure 10 shows an example of the case where the thin-plate approximation does not hold, but the theory can be applied in the time region where the diffusion depth of the current is shallow compared to the probe distance. The overall probe length is the same as before, but shorter probe separations of  $s_1 = 2 \text{ mm}$  and  $s_2 = 3 \text{ mm}$  are used. Since these values are similar to the plate thickness, a time dependent discrepancy between the approximate theory and the measured potential drop is expected according to figure 5.

The advantage of this approach, when applicable, is the simplicity of the thin-skin approximation especially on the form of (19). Furthermore, the steady state response can be analyzed separately by means of the DC formulas for a plate [19] and the material properties can be inferred without computing the response in the intermediate regime where the formulas are more complicated.

#### 3.5. Measurements on steel plates

Experimental data from measurements on the steel samples are shown in figure 11 for the 3 mm S235 steel plate and in figure 12 for the 1.2 mm steel sheet. The relative permeability and conductivity are calculated using (21) and (22) with the results  $\sigma = 3.6 \text{ MS m}^{-1}$ ,  $\mu_r = 61$  for the 3 mm steel plate and  $\sigma = 5.7 \text{ MS m}^{-1}$ ,  $\mu_r = 87$  for the 1.2 mm steel sheet.

Note that in both cases there is a discrepancy between the theory and measurements, reflecting the fact that no single value of  $\kappa$  results in an agreement over the entire range of the measured transients. Values of the fitting parameter  $\kappa$  were determined by minimizing the error in the late part of the decay where the transient approaches the steady state value. As a result, the theoretical calculations deviate from the experimental curves at short times. Similar results were reported previously for ACPD measurements on carbon steel plate [7] where by assuming a constant permeability, agreement with theory could only be obtained for low frequencies, whereas fitting the linear theory at higher frequencies requires the assumption of a frequency dependent relative permeability [20].

Although a value of the overall permeability is easily determined from the late decay of the transient, slightly lower values would be obtained from an analysis in the thin-skin regime. Likely factors contributing to this observation is the non-linear magnetization that is typical for ferromagnetic materials [21] and possibly slight inhomogeneity in the material.

## 4. Conclusions

In this work we have demonstrated the agreement between theory and experiment for four-point transient potential drop measurements on metal plates that are either thin compared to probe separation or when the analysis is restricted to a

thin-skin regime. As an addition to a similar previous theoretical study for the step response on plates we have included the response to a finite rise time of the drive current which is an important parameter in experimental applications.

In addition to the theoretical validation, we have demonstrated how the theory can be applied to rapidly determine the conductivity and permeability of conducting materials provided that the thickness is known. Moreover, in the case of non-magnetic materials whose relative permeability is known, a single transient measurement is sufficient to determine both the conductivity and the thickness.

The case of homogeneous plates considered here is a step towards the analysis and measurements on non-homogeneous materials with application to NDE of material properties that vary with depth and where the material may exhibit anisotropy for example due to applied stress or mechanical processing.

## Appendix

### A.1. Finite rise time for thin-skin approximation

In the thin-skin approximation the Laplace transform of the voltage is given by

$$v_{\text{ts}}(p) = \frac{\tilde{I}(p)}{2\pi\sigma} \sqrt{\mu\sigma p}.$$

Given an exponentially rising current, write its transform as

$$\tilde{I}(p) = \frac{I_0/\tau}{p(p + 1/\tau)}.$$

Now consider transforms on the form

$$f(p) = \frac{\sqrt{c}}{\sqrt{p}(p+c)},$$

noting that, after inserting for  $\tilde{I}(p)$ ,  $v_{\text{ts}}(p) \sim \sqrt{c}f(p)$  with  $c = 1/\tau$ . Rewrite  $f(p)$  in terms of the following partial fraction expansion [12],

$$f(p) = \frac{i}{2} \left[ \frac{1}{\sqrt{p}(\sqrt{p} + i\sqrt{c})} - \frac{1}{\sqrt{p}(\sqrt{p} - i\sqrt{c})} \right] \quad (\text{A.1})$$

where now the transform pair 29.3.43 in [17] can be used to invert the terms in the brackets according to

$$\frac{1}{\sqrt{p}(\sqrt{p} \pm i\sqrt{c})} \leftrightarrow e^{-ct} \operatorname{erfc}(\pm i\sqrt{ct}).$$

Inverting the terms in (A.1) and evaluating the sum gives

$$f(t) = e^{-ct} \operatorname{erfi}(\sqrt{ct}) \equiv \frac{2}{\sqrt{\pi}} D(\sqrt{ct}),$$

where we have used the relation  $\operatorname{erfc}(ix) - \operatorname{erfc}(-ix) = -2\operatorname{erf}(ix)$  and the imaginary error function  $\operatorname{erfi}(x) = -i\operatorname{erf}(ix)$ . The above equation is the definition of the Dawson function  $D(x)$  introduced in the main text, otherwise known as Dawson's integral, and can be evaluated numerically<sup>2</sup>.

<sup>2</sup> An implementation of the Dawson function is readily available in the open source scientific Python library SciPy [22].

## ORCID iDs

Øyvind Persvik  <https://orcid.org/0000-0002-2698-6125>

## References

- [1] Miccoli I, Edler F, Pfnür H and Tegenkamp C 2015 The 100th anniversary of the four-point probe technique: the role of probe geometries in isotropic and anisotropic systems *J. Phys.: Condens. Matter* **27** 223201
- [2] Bowler N 2011 Four-point potential drop measurements for materials characterization *Meas. Sci. Technol.* **22** 012001
- [3] Pettersen S R, Stokkeland A E, Kristiansen H, Njagi J, Redford K, Goia D V, Zhang Z and He J 2016 Electrical four-point probing of spherical metallic thin films coated onto micron sized polymer particles *Appl. Phys. Lett.* **109** 043103
- [4] Zangwill A 2013 *Modern Electrodynamics* (Cambridge: Cambridge University Press)
- [5] Merah N 2003 Detecting and measuring flaws using electric potential techniques *J. Qual. Maint. Eng.* **9** 160–75
- [6] Saguy H and Rittel D 2007 Flaw detection in metals by the ACPD technique: theory and experiments *NDT & E Int.* **40** 505–9
- [7] Bowler N and Huang Y 2005 Model-based characterization of homogeneous metal plates by four-point alternating current potential drop measurements *IEEE Trans. Magn.* **41** 2102–10
- [8] Bowler J R and Bowler N 2007 Theory of four-point alternating current potential drop measurements on conductive plates *Proc. R. Soc. A* **463** 817–36
- [9] Sposito G, Cawley P and Nagy P B 2010 Potential drop mapping for the monitoring of corrosion or erosion *NDT & E Int.* **43** 394–402
- [10] Corcoran J and Nagy P B 2018 Magnetic stress monitoring using a directional potential drop technique *J. Nondestruct. Eval.* **37** 60
- [11] Hognestad H and Honne A 1998 Determination of stress in ferromagnetic steel by potential drop measurements *Mater. Sci. Tech.* **14** 1109–14
- [12] Bowler J R 2011 Evaluation of the transient potential drop of a four-point probe *Appl. Phys. Lett.* **98** 264105
- [13] Persvik Ø and Bowler J R 2017 Evaluation of four-point transient potential drop on conductive plates *Appl. Phys. Lett.* **110** 084102
- [14] Yilmaz S 2015 The geometric resistivity correction factor for several geometrical samples *J. Semicond.* **36** 082001
- [15] Knoepfel H E 2000 *Magnetic Fields: A Comprehensive Theoretical Treatise for Practical Use* (New York: Wiley)
- [16] Boas M L 2006 *Mathematical Methods in The Physical Sciences* (New York: Wiley)
- [17] Abramowitz M and Stegun I A 1972 *Handbook of Mathematical Functions with Formulas, Graphs, and Mathematical Tables* (New York: Dover)
- [18] Theodoulidis T P and Bowler J R 2005 The truncated region eigenfunction expansion method for the solution of boundary value problems in Eddy current nondestructive evaluation *AIP Conf. Proc.* **760** 403–8
- [19] Lu Y, Bowler N, Bowler J R and Huang Y 2009 Edge effects in four-point direct current potential drop measurements on metal plates *J. Phys. D: Appl. Phys.* **42** 135004
- [20] Bowler N 2006 Frequency-dependence of relative permeability in steel *AIP Conf. Proc.* **820** 1269
- [21] Cullity B and Graham C 2009 *Introduction to Magnetic Materials* 2nd edn (New York: Wiley)
- [22] Jones E *et al* 2001 SciPy: Open source scientific tools for Python (<http://scipy.org/>)